MAGNETOUR: Surfing Planetary Systems on Electromagnetic and Multi-Body Gravity Fields

Gregory Lantoine[1]
Jet Propulsion Laboratory, California Institute of Technology, Pasadena, CA, 91109, U.S.A

Ryan P. Russell[2]
University of Texas at Austin, Austin, TX 78712-1221, U.S.A

and

Rodney L. Anderson[3], Henry B. Garrett[4] and Ira Katz[5]
Jet Propulsion Laboratory, California Institute of Technology, Pasadena, CA, 91109, U.S.A

A comprehensive tour of the complex outer planet systems is a central goal in space science. However, orbiting multiple moons of the same planet would be extremely prohibitive using traditional propulsion and power technologies. In this paper, a new mission concept, named Magnetour, is presented to facilitate the exploration of outer planet systems and address both power and propulsion challenges. This approach would enable a single spacecraft to orbit and travel between multiple moons of an outer planet, without significant propellant or onboard power source. To achieve this free-lunch 'Grand Tour', Magnetour exploits the unexplored combination of magnetic and multi-body gravitational fields of planetary systems, with a unique focus on using a bare electrodynamic tether for power and propulsion. Preliminary results indicate that the Magnetour concept is sound and is potentially highly promising at Jupiter.

I. Introduction

A full study of the giant, complex outer planet systems is a central goal in space science. Exploring these systems can help us understand better our solar system as a whole. According to the Decadal Survey,[1] a full exploration of planetary moon systems of Jupiter, Saturn and Uranus are top priorities for the next flagship class tour and orbiting mission. In particular, a comprehensive visit of the four large moons of Jupiter, known as the "Galilean moons", is important to search for liquid water and extraterrestrial life.

However, all outer planet missions must face tough engineering challenges. Propulsion needs have particularly been a critical issue. The Galileo and Cassini missions have been successful but "handcuffed" missions. The large propellant required by traditional chemical propulsion for capture and tour maneuvers constrained their science return by limiting scientific payload. In addition, intrinsic fuel limitations have hampered long-term, more detailed scientific study of the moons. Orbiting multiple moons would especially be too prohibitive with traditional propulsion. Outer planet exploration is also handicapped by scarcity of power. The low solar luminosity makes the use of solar arrays difficult (for instance, the solar intensity at Jupiter is only one twenty-fifth of its value at Earth), and radioisotope power systems (RPS) provide generally low levels of power per unit and require large masses, which (as with chemical propellant mass) can limit the mission scientific payload. Moreover RPS units are currently produced at a low annual rate and are relatively expensive. Space nuclear power is another option. The Jovian Icy Moons Orbiter (JIMO) concept would have used a nuclear reactor system for both power and powering high specific-impulse electrical thrusters, but the mission was canceled when the estimated cost became prohibitive. In an

[1] Mission Design Engineer, Mission Design & Navigation Section, gregory.lantoine@jpl.nasa.gov.
[2] Associate Professor, Department of Aerospace Engineering and Engineering Mechanics, ryan.russell@utexas.edu.
[3] Technologist, Mission Design & Navigation Section, Rodney.L.Anderson@jpl.nasa.gov.
[4] Principal Scientist, Reliability Engineering & Mission Environmental Assurance, Henry.B.Garrett@jpl.nasa.gov.
[5] Group Supervisor, Advanced Propulsion Group, Ira.Katz@jpl.nasa.gov.

uncertain NASA budget climate, there is therefore an urgent need for new ideas that could overcome these issues under a reasonable cost. The development of revolutionary space technologies is critical to explore outer planets more effectively.

In this paper, a new mission concept, named Magnetour, is proposed to facilitate the exploration of outer planet systems and address both power and propulsion challenges. This concept would enable a single spacecraft to orbit and travel between multiple moons of an outer planet, with no propellant nor onboard power source required. To achieve this free-lunch 'Grand Tour', the unexplored combination of magnetic and multi-body gravitational fields of planetary systems is exploited, with a unique focus on using a bare tether for power and propulsion. The concept was originated by a NIAC Phase One study. The full details of the NIAC study can be found in the corresponding final report.[2]

This paper summarizes the results and findings of the NIAC Phase One study, and is organized as follows. First, an overview of the Magnetour mission concept is presented. Then the performances of electrodynamic tethers and other electromagnetic systems are assessed in the Jovian environment. In addition, a spacecraft configuration is presented that fully incorporates the tether in the design. A method to exploit the coupled behavior of magnetic and multi-body gravitational dynamics is given next. A propellantless trajectory baseline capable of orbiting multiple moons at Jupiter is designed to confirm the feasibility of the concept and gain further insight in the benefits of Magnetour. Finally risks and challenges of Magnetour are discussed.

II. Magnetour Concept Overview

The Magnetour concept is a NIAC Phase One study to find innovative technologies for enabling multi-moon outer planet missions. In the Magnetour concept (see Figure 1), a propellantless spacecraft could orbit several of the moons of any one of the outer planets, allowing for long-duration observations. For example, a multi-moon orbiter could explore Jupiter's planet-sized and likely water-bearing moons - Callisto, Ganymede and Europa - one after the other. Classical propulsion methods would require a prohibitive amount fuel to perform this type of mission. To make this "free-lunch" tour feasible, the Magnetour concept relies on two advances.

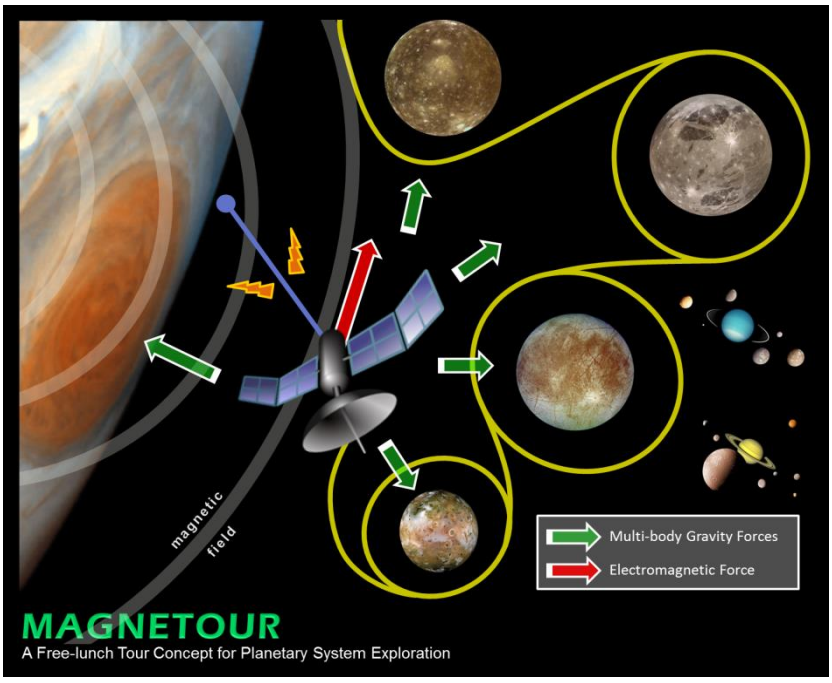

Figure 1. Overview of the Magnetour concept

First, this concept involves a very low delta-v tour of planetary moons by taking advantage of full, natural dynamics to efficiently navigate in space rather than 'fighting' the dynamics with thrusting. This innovative space travel technique is called the Intermoon Superhighway.[3] In this framework, the cost of inserting and orbiting the moons is also reduced via weakly captured orbits, such as Lyapunov and Halo orbits, that act as destination science orbits and waypoints to the next moon. This approach is a dramatic departure from traditional patched conics and therefore cannot be explained using two body mechanics, the driver for traditional planetary moon tours. Until

recently, these efficient trajectories were undiscovered, and mission designers were simply unaware that such path planning options were physically achievable.

Secondly, instead of using conventional chemical propulsion, the Magnetour concept uses an electrodynamic tether (a conductive long and thin tape) as a revolutionary means for performing the required low delta-v maneuvers of our low-energy tour. The tether forces can be also conveniently used for the critical planetary capture phase. As the tether travels through the planetary magnetic field, interactions between the surrounding plasmasphere and tether can produce an electromagnetic Lorentz force that can be exploited to change the orbital profile. The electromagnetic system could also serve as its own power source by plugging in an electric load where convenient; in particular a large energy could be tapped from the big power developed during capture, with negligible effect on the dynamics. By switching on and off the electromagnetic system in specifically designed sequences, the orbit could be made to evolve without recourse to propellant and on-board power sources. A low-energy planetary tour, involving navigation through the moon system and gravitational capture, would therefore offer a perfect opportunity to exploit this idea. While this application is particularly promising in the Jovian system where the magnetic field is rotating fast and is exceptionally strong, the proposed concept could benefit future missions to any of the gas giant moon systems.

The MAGNETOUR mission concept can be decomposed in different phases (see Figure 2). The tour starts with a critical planetary capture into an equatorial, highly elliptical orbit. The electromagnetic system is activated to brake the spacecraft at closest approach. At Jupiter, this operation can save between 0.5 and 2 km/s of delta-v over classical chemical approaches (in Galileo's case, 371 kg of fuel).[4] In the second phase (Apojove Pump Down), repeated application of the electromagnetic force, at constant perijove vicinity, can progressively lower the apojove. Flybys of the moons can be made during this phase. Once the apojove reaches a moon of interest for capture, high-velocity flybys of the moons are made to reduce the eccentricity and raise periojove (Perijove Pump Up). Then multi-body effects and small Lorentz force maneuvers are used to gravitationally capture and transfer between moons ('InterMoon Superhighway'). This paper is focused on the last phase, i.e. a low energy, multi-moon tour. In the full NIAC Phase 1 study, trajectory options for each phase were considered, and details can be found in Ref. 2 and Ref. 5.

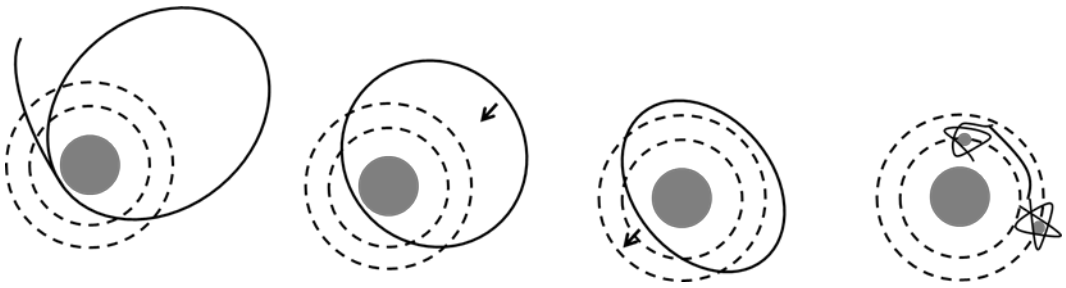

Figure 2. Phases of MAGNETOUR: left to right: Capture; Apojove Pump Down; Perijove Pump Up; and Low-energy inter-moon transfer (InterMoon Superhighway) and loosely captured orbits.

III. Selecting and Modeling Electromagnetic Systems

Trade studies are performed to select and assess appropriate electromagnetic systems for Magnetour. First an analysis of the performance of electrodynamic tether systems is conducted. Simplified models for the electrodynamic tethers are formulated to provide theoretical estimates of the concept expected performance. Then investigating further electrostatic tether systems is suggested. Finally, a brief discussion on other electromagnetic systems is given, explaining why they would not be efficient.

A. Electrodynamic tether

Electrodynamic tethers (EDTs) are bare (uninsulated), conducting wire or tape tethers terminated at one end by a plasma contactor. These tethers could provide both power and propulsion, with just tether hardware accounting for tether subsystem mass. In this subsection, the propulsion and power performance of an EDT are evaluated as a function of tether length.

1. Lorentz force & power

The electrodynamic tether uses two basic electromagnetic principles to its advantage. The first principle is that of voltage induction. Basically, as the tether moves through a magnetic field $\boldsymbol{B}$, the electric charges contained inside the tether experience a motional electric field $\boldsymbol{E}_m$ in the orbiting tether frame:

$$E_m = v_{rel} \times B \tag{1}$$

where $\boldsymbol{v}_{rel}$ is the relative velocity of spacecraft with respect to the co-rotating plasma. This electric field acts to create a potential difference across the tether by making the upper end of the tether positive with respect to the lower end. The basic requirement for producing a current from this potential difference is establishing effective contact, both anodic and cathodic, with the ambient plasma. Hollow cathodes are used to emit electrons at the cathodic end. The anodic contact is provided by the tether itself that is left bare of insulation, allowing it to collect electrons over the segment coming out polarized positive, as a giant cylindrical Langmuir probe in the orbital-motion-limited (OML) regime.[6] Electrons can then enter and exit the tether into the surrounding plasma, closing a circuit and thereby enabling the voltage present to drive a current along the tether. From Ref. 7, the resulting length-averaged electric current vector, $\boldsymbol{I}_{av}$, through a perfect conducting tether of length, L, and width, w, is:

$$I_{av} = \frac{2}{5}\frac{2wL}{\pi} eN_e \sqrt{\frac{2eE_tL}{m_e}}\hat{u} \tag{2}$$

where $\hat{\boldsymbol{u}}$ is the unit vector along the tether, N_e is the plasma density, m_e is the mass of an electron, and $E_t = \boldsymbol{E_m} \cdot \hat{\boldsymbol{u}}$ is the projection of the motional electric field E_m along the tether. It follows that an electromagnetic force, called the Lorentz force, acts on the tether and arises from the interactions of this electric current with the magnetic field of the planet:

$$F_L = LI_{av} \times B \tag{3}$$

Note that if the plasmasphere rotates faster than the spacecraft ($v_{rel} < 0$), this force produces thrust. On the other hand, if the spacecraft travels faster than the magnetic field, this force is a drag on the spacecraft/tether system. For a tether oriented perpendicular to the magnetic field, the magnitude of the Lorentz force can be simply expressed as:

$$F_L = LI_{av}\, B \tag{4}$$

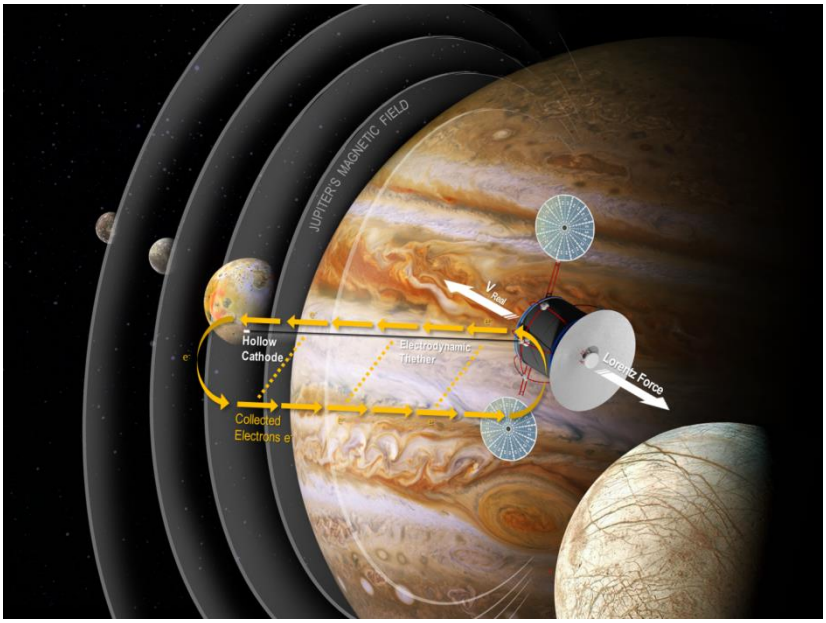

Figure 3. Principle of bare electrodynamic tether

This mechanism explains how an electrodynamic tether can be used for propulsion. This process is illustrated in Figure 3 (in the figure the force is a drag). Note that the magnitude of the Lorentz force varies along a trajectory with a nonlinear dependence on position and velocity, which will make the trajectory design challenging. However, it is possible to control the tether current by adding a resistor or by switching off at convenience the Hollow cathode.

In addition to propulsion, the tether can also serve as power source whenever an electric load is plugged in its circuit. The magnitude of the generated power can be expressed in terms of the electromotive force as:

$$P_L = E_t L I_{av} \quad (5)$$

The deployment and Lorentz effects of long electrodynamic tethers were demonstrated by several demo flight missions.[8,9] The SEDS-I and SEDS-II missions successfully deployed 20-km and 7-km non-conductive tethers in 1993 and 1994. Also in 1993, the plasma motor generator (PMG) experiment demonstrated the electron collection and current flowing by a tethered system. Later, in 1996, the TSS-1R mission, despite ending prematurely by an electrical arc that severed the tether, experienced a 0.4 N electrodynamic drag.

The magnetic field and plasmas around a planet play a key role in computing the forces on a tether. The four outer planets in the solar system have been observed to have strong magnetic fields, substantial plasma environments, and trapped radiation belts. Table 1 compares the physical properties and magnetic fields of Jupiter, Saturn, Uranus, and Neptune. While about 1/3 to 1/2 the size of Jupiter and Saturn, Uranus and Neptune are very different in one very significant way from these planets — their magnetic fields are significantly tilted with respects to their spin axes. These complex magnetic and spin axis alignments lead to correspondingly complex magnetic fields which in turn complicated interactions with a tether. The effects of these magnetic field variations on tethers pose a particularly challenging orbital analysis and will not be investigated in this paper.

Table 1. Physical and magnetic properties of the 4 gas giants.[10]

PHYSICAL PROPERTIES:	Jupiter	Saturn	Uranus	Neptune
Equatorial radius (km)	71492	60268	25559	24766
GM ($km^3 s^{-2}$)	126686537	37931284.5	7793947	6835107
Mass (kg)	1.8986E+27	5.68461037E+26	8.6832E+25	1.0243E+26
Density (gm cm^{-3})	1.326	0.687	1.318	1.638
DIPOLE CHARACTERISTICS:	**Jupiter**	**Saturn**	**Uranus**	**Neptune**
Dipole tilt (deg)	9.6	0	58.6	47
Dipole offset (rp)	0.131	0.04	0.3	0.55
Magnetic moment (gauss R_p^3)	4.28	0.21	0.228	0.133

For reference, Jupiter and Saturn are roughly 10 times the size of the Earth while their magnetic moments are ~$2x10^4$and ~10^3 larger. As the magnetic field at the equator of a planet is proportional to the magnetic moment divided by the cube of the radial distance, Saturn's magnetic field/magnetosphere is proportional to Earth's while Jupiter's magnetic field/magnetosphere is 20 times larger than the Earth's and Saturn's. As the maximum energy and flux levels of trapped particles in a magnetosphere are proportional to the magnetic field strength, the Jovian system can maintain much higher particle energies than those at Saturn and the Earth. Because of the exceptional strength of the magnetic field of Jupiter, the Jovian system is particularly appropriate for the use of electrodynamic tethers. The rest of the paper will therefore mainly focus on the Jovian system.

From Eq. 4 and Eq.5, the capability of electrodynamic tethers in a circular orbit around Jupiter is determined by computing the Lorentz force and power produced as a function of orbital radius and tether length (see Figure 4). The estimated averaged electrical current along the tether is also given (see Figure 5). This preliminary analysis was limited to simple physical models: the magnetic field was assumed to be perfect dipole (good approximation close to Jupiter), the electron density N_e was derived from a piecewise constant approximation of the Divine and Garrett model,[11] and the tether-spacecraft system was treated as point mass. A nominal tether width of 1 cm is assumed. Note that the power data are ideal and do not include losses.

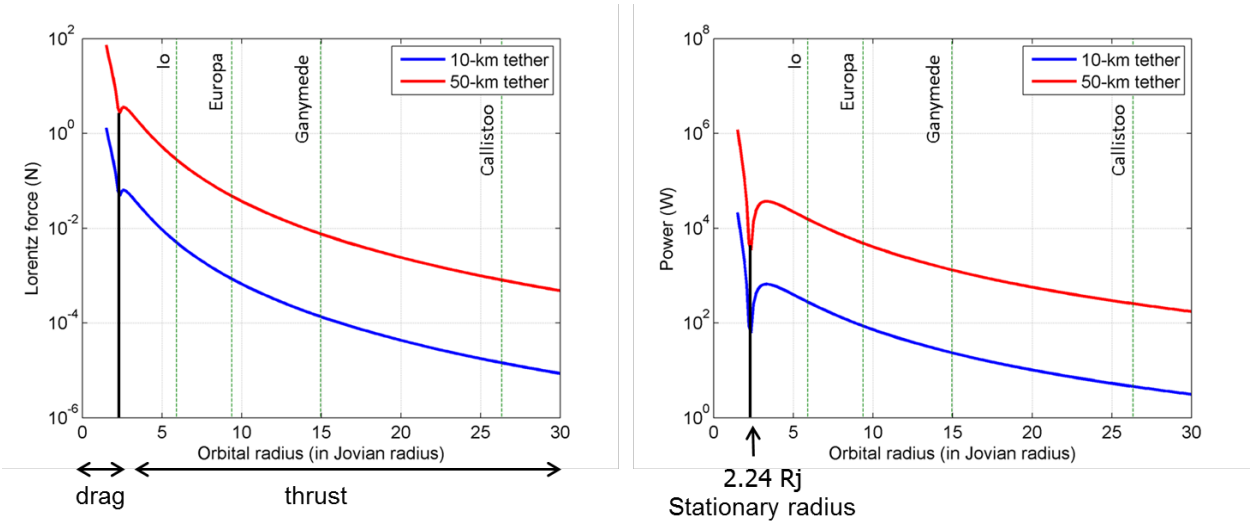

Figure 4. Lorentz force and Power vs orbital radius

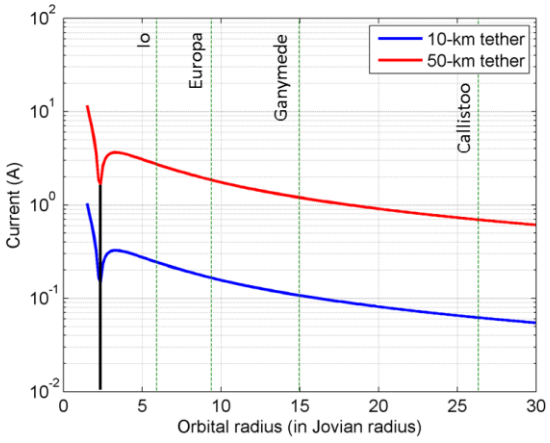

Figure 5. Current vs orbital radius

A tether between 10-km and 50-km long[6] could provide between 1 kW and 1 MW of power at Io and below, while producing a force between 0.01 N and 100 N. An electrodynamic tether has therefore the ability to significantly change the trajectory and power the spacecraft at Io and the other Jovian moonlets. However, farther from Jupiter, in the Ganymede and Callisto regions, the magnetic field is much weaker and therefore the resulting thrust and power experience a significant drop. Without additional propulsion and power options, in these farther regions, the spacecraft therefore needs to be operated under low power conditions and can perform only small maneuvers. A 10-km tether is clearly the lower limit to obtain decent forces and power and the Galilean moons. Examples of Lorentz force magnitudes for a 50-km tether are: 100 N (for drag) in low Jovian orbit; and 0.5, 0.05, 0.01, 0.001 N (for thrust) at Io, Europa, Ganymede and Callisto, respectively.

2. Tether design & mass

A tape tether design has been selected since it has a more favorable geometry for current collection and micrometeoroid survivability compared to 'traditional' wire tethers.[12] While a tape is more likely to be hit, a micrometeoroid would only punch a hole in it and not sever it. In addition, the tether requires a material with low density, as well as good conductive and mechanical properties. Other factors that must be considered are ease of manufacturing, cost, and radiation shielding properties. A comparison of some conductive tether materials is given in Table 2.

[6] Note that a 50-km long tether is not unrealistic: for instance, in 2007 a 31-km long tether was successfully deployed in LEO during the YES2 spacemail mission.[13]

Table 2. Properties of candidate tether conductive materials

Material	Density ρ (kg/m^3)	Specific conductivity (m^2/Ω.kg)	Tensile strength (MPa)
Aluminum	2700	13500	276
Silver-clad Aracon	3200	2325	1020
Beryllium	1850	16630	550

The corresponding tape tether mass can be estimated for a given tether density ρ, length L, width w and thickness t by :

$$m = \rho w L t \quad (6)$$

Since the thickness t does not appear in the Lorentz force equation (Eq. 4), in order to minimize mass, a value of t as small as possible must be chosen. Currently a thickness of 0.05 mm is feasible,[14] which is the value we selected in this study. Using the material densities of Table 2 and the same width as in the previous subsection (1 cm), the resulting tether mass was computed as a function of tether length for Aluminum, Aracon, and Beryllium.

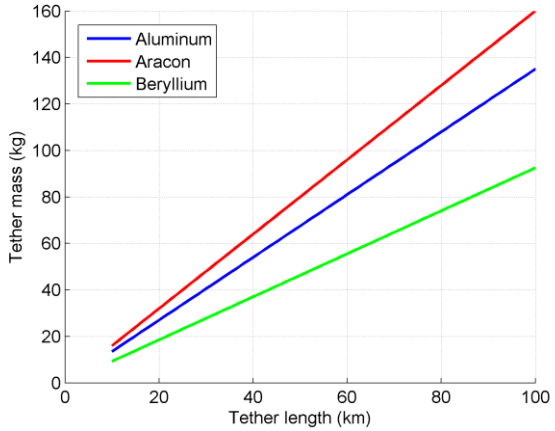

Figure 6. Tether mass vs tether length for different materials

From Table 2, the optimum choice of material would be Beryllium. This material has the highest specific conductivity and lowest density, with a good tensile strength. Unfortunately, highly ductile alloys of beryllium have not been found, so it is difficult to make it into a tape form. As a result, because of its high specific conductivity, low cost, availability, good radiation shielding properties, and ready available inductile form, the electrodynamic tether is assumed to be made of aluminum in this study.

3. Hollow cathode

Hollow Cathodes are commonly used as electron emitters with electrodynamic tethers. Laboratory experiments at JPL[15] suggest that a standard hollow cathode can provide up to 10 mN of thrust if sufficient power is provided (see Figure 7). A hollow cathode can therefore have an interesting dual use: an electron emitter, *and* a standalone mini-thruster (albeit with low thrust and Isp). This additional thruster could be used as

1. complementary low-thrust propulsion: to supplement the Lorentz force when small and provide additional degrees of freedom in thrust directions
2. attitude control and tether stabilization system

Future work needs to investigate the effect of hollow cathode thrusting on tether stability and a quantification of the benefits of a hollow cathode thruster on a Magnetour mission.

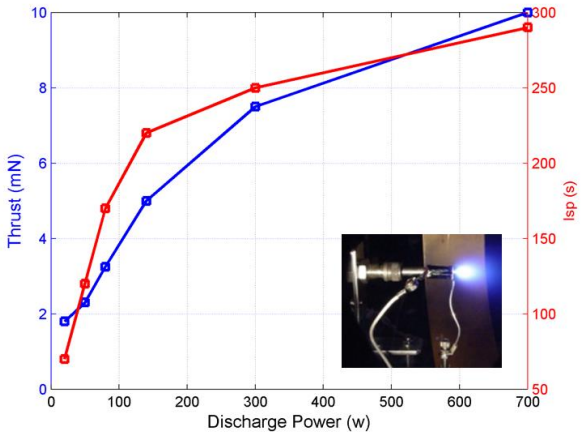

Figure 7. Hollow cathode thrust and Isp vs power

4. Comparison with competing standard technologies

Electrodynamic tethers compare favorably to other propulsion and power source systems. These tethers can provide high thrust and extremely high specific impulse performance, as well as high power-to-mass ratios (see Figure 8). Electrodynamic tethers are therefore a critical technology for Magnetour in that they overcome the fundamental limitations of propellant-based propulsion systems.

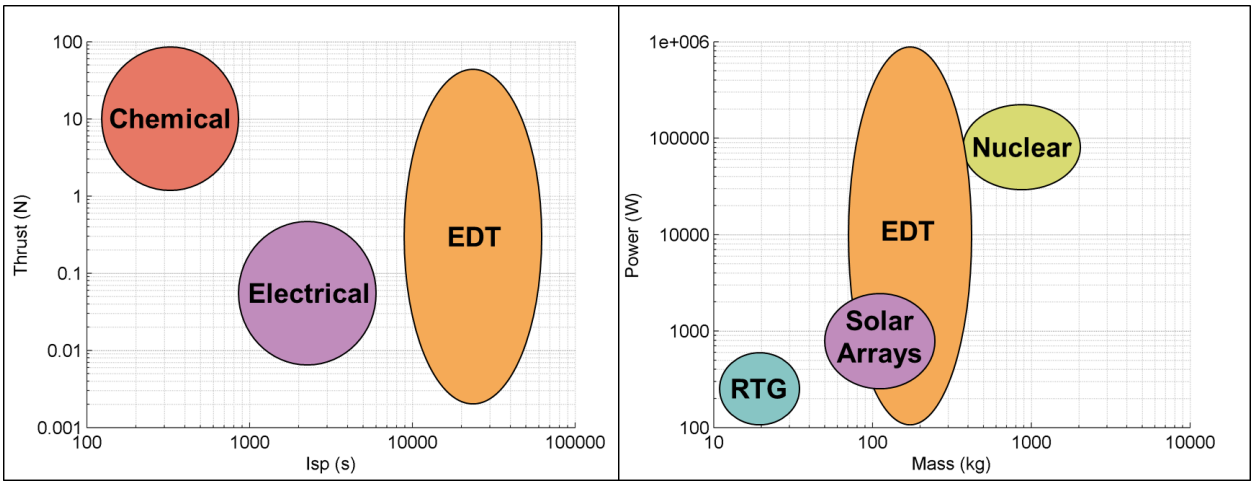

Figure 8. Comparison of EDTs with other propulsion and power technologies

B. Electrostatic tether

Close to the planet, it was showed that electrodynamic tethers can provide sufficient thrust and power given enough length (see Figure 4). However, when the distance increases, the capability of electrodynamic tethers drops significantly. In addition, before planetary capture, delta-v and power capability would be needed for trajectory correction maneuvers during the interplanetary trip, when the Lorentz force is not available. In such cases, an electrostatic tether is a promising alternative. In fact, as well as using the electromagnetic force to generate thrust, it is also possible to use bare wire tethers to generate thrust using electrostatics. Recent work for the NIAC program by former Chief Technologist Mason Peck suggested the possibility of propelling a spacecraft with the Lorentz force component of the solar wind electric field.[16] In addition Janhunaen has shown that electrostatically repelling the ions of the solar wind using bare wire tethers can be quite efficient.[17-19] This concept could be exploited both for ions in the solar wind and ions in Jupiter's ionosphere and magnetosphere.

The ion electrostatic propulsion concept utilizes the fact that the potential that repels ions drops off from a wire logarithmically with radius until Debye shielding becomes important, while the orbit limited electron current collection radius drops off more quickly, with the square root of the potential. For typical solar wind conditions at 1

AU, a spinning electrostatic sail of 10 micron radius wires held at 2000 V could generate 2 Nt per kW of solar array electrical power. The Coulomb thrust is here dominant against the Lorentz thrust.

Since both electromagnetic and electrostatic tether propulsion concepts make use of the same bare wire tether hardware, combining the two propulsion schemes could provide spacecraft thrust in regions of space where the ambient magnetic field is small, but the ion flux is large as well as vice versa. This additional flexibility could greatly improve the Magnetour performance. In future work, investigating in more detail the electrodynamic – electrostatic dual mode of bare tethers is strongly recommended.

C. Limitations of other electromagnetic systems

Another way to alter a spacecraft path through the Lorentz force is by storing a net electrical charge on a surface of a conducting sphere that would encompass the spacecraft. The electrical charge would be maintained by electron-beam emission.[16] However, the capacitance of a sphere of radius R is $4\pi R$, which corresponds to about 10-10 F for a meter spacecraft. It follows that, for a spacecraft with a charge of 1 C, the potential would be 1010 V. This potential level would be challenging to maintain at Jupiter without providing large power.

Another different idea is to carry an electromagnetic "hoop" which you can use as a giant magnetosphere to interact with the planetary magnetic field torques or help with capture.[20] However, maneuvers are more limited because such a system could only be attracted towards the magnetosphere's poles or repelled from them. This system has also a much lower TRL than electrodynamic tethers.

IV. Spacecraft Configuration

Figure 9 – Figure 12 illustrate a preliminary, non-optimized configuration for a Magnetour spacecraft. This configuration was determined after performing an initial layout of the spacecraft using CAD models (with real dimensions) of all the systems and components needed. Most of the configuration is based on the cable that needs to be stored and deployed. The cylindrical section constitutes the core the space spacecraft. This part provides extra radiation shielding capabilities while the cable is still rolled and it is can be parametrically change in size during the design stage. As a result the dimension of the spinning barrel can be adapted allowing always an interior volume for flight systems, electronics, instruments equipment, etc. as well as front part (exposing instruments toward the target) and a back part for a HGA antenna. Dimensions can be adapted easily to the spatial requirements of the mission and launch. Deployable like solar arrays as well as other antennas etc. can be attached on the edges having all the circular section for the stowed state. Even if the tether is used as a power source, solar panels are needed for the interplanetary cruise.

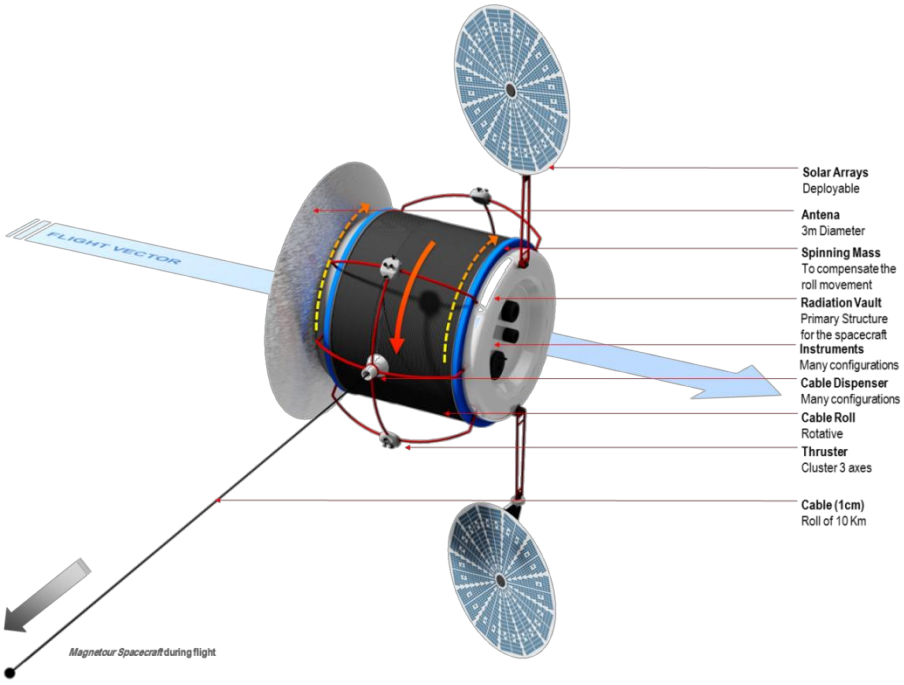

Figure 9. External view of proposed spacecraft configuration

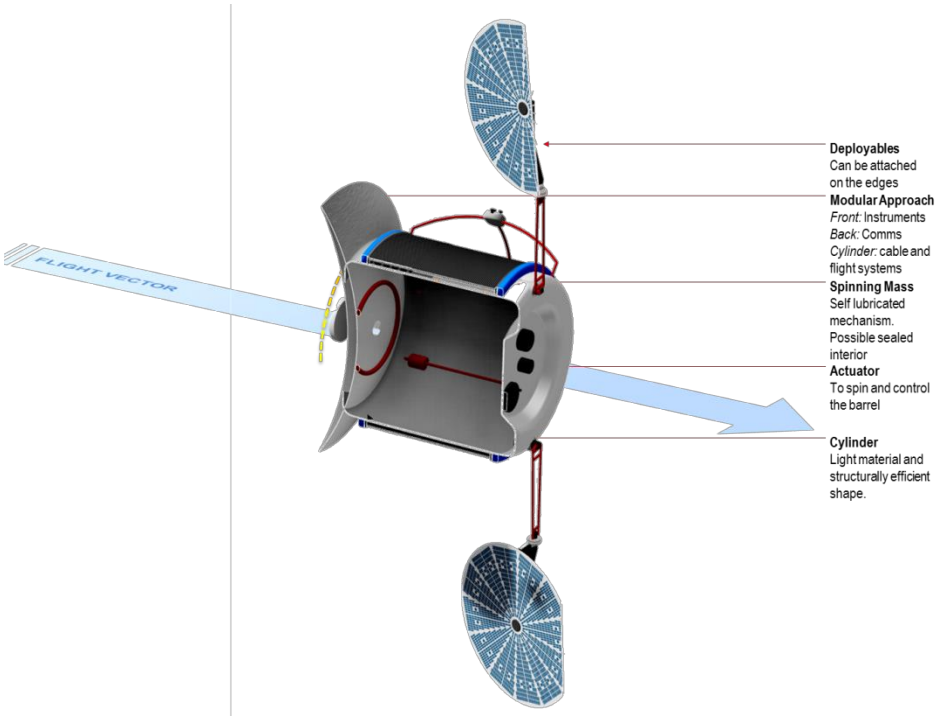

Figure 10. Sectioned view of proposed spacecraft configuration (1)

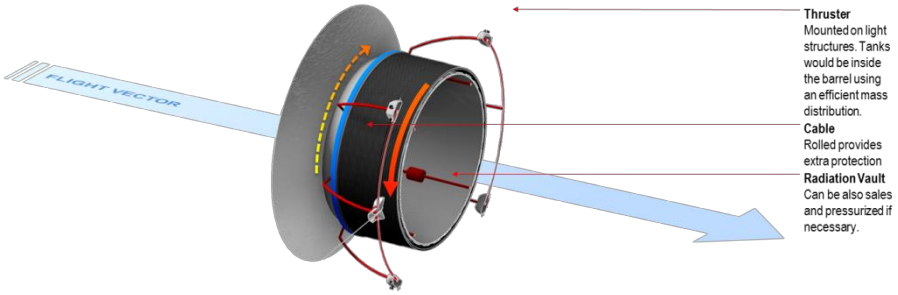

Figure 11. Sectioned view of proposed spacecraft configuration (2)

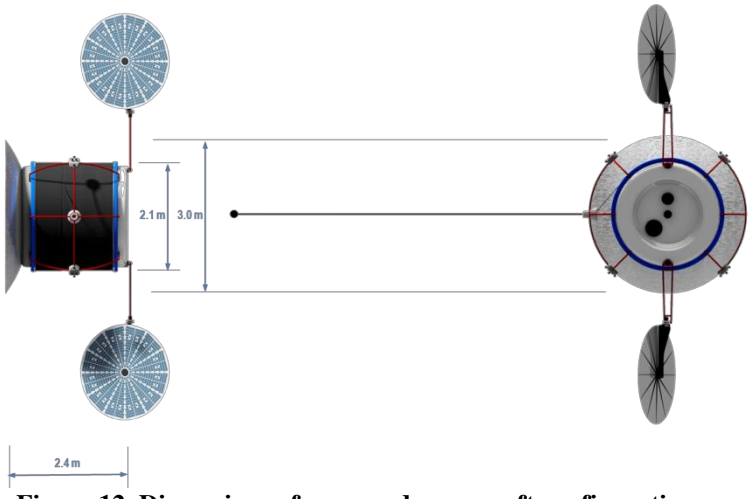

Figure 12. Dimensions of proposed spacecraft configuration

A preliminary analysis was carried out to determine the amount of radiation shielding provided by a partially-deployed tether. Table 3 shows the number of rolls and layers needed based on the geometry of the roll and the cable. If a 10km cable is used with 1 km already deployed of a 1cm radius cable (should be less) this shows how much volume of cable is still rolled in the spacecraft. Knowing the volume and the density we can know the mass of the cylinder of cable around the spacecraft.

Table 3. Tether volume available for radiation shielding protection for partially-deployed tether

Layer	Rolls	Rolled Length (cm)	Remaining Cable (cm)	Volume of Cable (cm3)	Mass of Cable (Kg)	1 Roll Length (cm)	Max Length (cm) per layer
1	150	95190.26	804809.74	299049.01	2392.39	634.60	95190.26
2	150	96132.74	708677.01	302009.89	2416.08	640.88	96132.74
3	150	97075.21	611601.79	304970.78	2439.77	647.17	97075.21
4	150	98017.69	513584.10	307931.66	2463.45	653.45	98017.69
5	150	98960.17	414623.94	310892.54	2487.14	659.73	98960.17
6	150	99902.65	314721.29	313853.42	2510.83	666.02	99902.65
7	150	100845.12	213876.16	316814.30	2534.51	672.30	100845.12
8	150	101787.60	112088.56	319775.18	2558.20	678.58	101787.60
9	150	102730.08	9358.48	322736.06	2581.89	684.87	102730.08
10	14	9358.48	0.00	29400.54	235.20	691.15	103672.56

V. Tether-Assisted Multi-Moon Tour Design

The technical and programmatic feasibility of Magnetour is assessed on a reference mission. Since the concept is particulary promising at Jupiter (see section III.3.1), a preliminary trajectory design is performed on a Jovian multi-moon mission using simplified models for the gravitational and magnetic fields.

A. Exploiting the InterMoon Superhighway

Recent applications of dynamical systems theory to the multi-body astrodynamics problem have led to a new paradigm of intermoon trajectory design.[3,21-25] From this perspective, trajectories can take advantage of natural dynamics to efficiently navigate in space rather than 'fighting' the dynamics with thrusting. In the same way as sailing ships use winds and currents to travel the oceans, a spacecraft could use the gravity and movement of the planet and its moons to travel in planetary systems. Through the explicit use of the low-energy transport mechanisms in the three-body gravitational problem, it is possible to systematically take advantage of the chaotic design space between planetary moons to reduce dramatically the delta-v required to transfer between weakly captured orbits of different moons. This so-called 'InterMoon Superhighway' approach is based on using unstable resonant periodic orbits and their associated manifolds in order to effectively 'steer' through the chaotic resonant transitions through high altitude three-body flybys (see Figure 13). Magnetour could clearly benefit from this approach. A spacecraft could, for example, transfer (with little delta-v needed) between a weakly captured Lyapunov orbit at Ganymede and a weakly captured Lyapunov orbit at Europa.

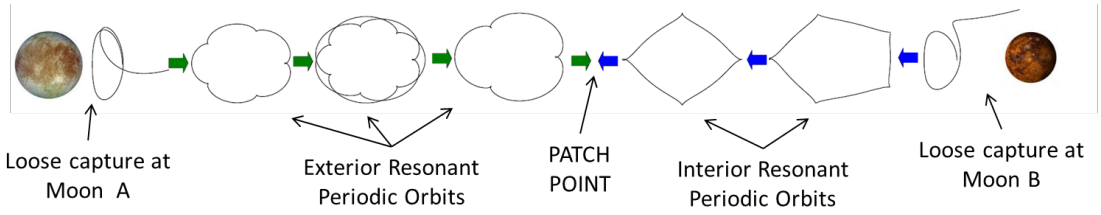

Figure 13. The InterMoon Superhighway trajectory concept goes through multiple orbital resonances with the moons to achieve low delta-v transfer between planetary moons

This dynamical mechanism of 'resonance hopping' can be visualized by numerically integrating several initial random points in an unstable region close to one of the moons. The dotted background of Figure 14 shows the evolution of the trajectories in phase space (semi-major axis a vs. argument of periapsis w) after starting close to Ganymede. This phase space reveals the resonance structure which governs transport from one orbit to another. The random scattered points correspond to chaotic motion whereas blank `holes' represent stable resonant islands. For every semi-major axis value corresponding to a K:L resonance, there is a band of L islands. It has been shown that there exists an unstable periodic orbit in the chaotic zone between each island.[26] This observation explains why unstable resonant orbits are so important, they are similar to passes (or waypoints) in the chaotic environment, which have to be crossed in order to move in the phase space without getting stuck in stable resonances. For connecting two distant points, it is therefore necessary to cross a certain number of resonances. For instance, the large dots in

Figure 14 give one possible solution that jumps between resonant bands. This mechanism can therefore help us navigate the chaotic three-body design space and design efficient trajectories.

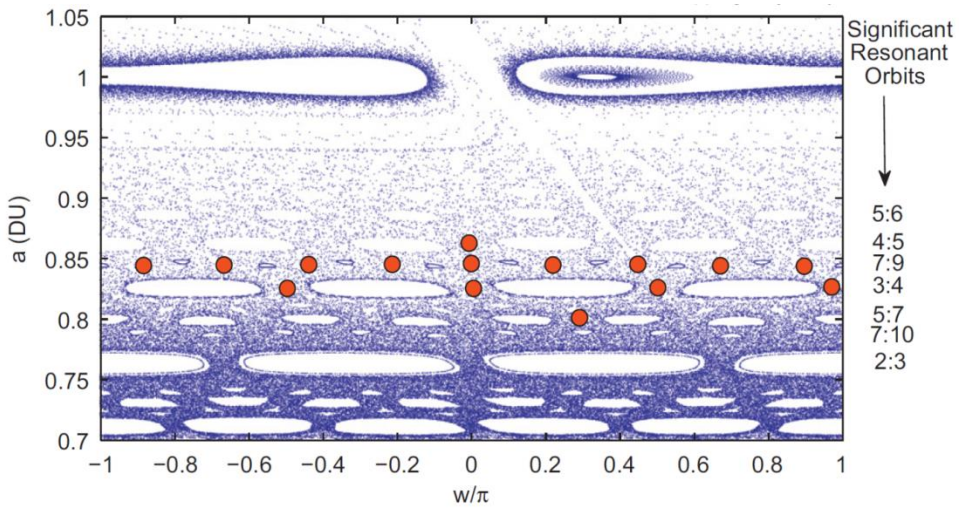

Figure 14. Phase space of the Jupiter-Ganymede three-body problem illustrating the resonant islands and the transport mechanism

B. Tether-assisted trajectory optimization

This low-energy approach to the transport between moons relies on the chaotic dynamics of the three-body problem, and is therefore extremely challenging to design. Adding tether maneuvers increases even more the complexity, especially since the thrust provided by the tether is small (see section III.3.1) and the thrust direction is not free (depending on magnetic field and tether attitude orientations). However, this property also offers a unique opportunity to combine the low thrust control of the sail with the sensitive dynamics of the InterMoon Superhighway to provide mission design options not available with conic orbits. In order to exploit these sensitive dynamics, new tools are therefore needed to construct and optimize three-body trajectories with tether maneuvers.

A direct, multiple shooting approach is proposed. The multiple shooting method attempts to limit the sensitivity issue by splitting the integration interval to reduce error propagation. Additional matching constraints are then imposed to get a continuous solution on the whole interval. This strategy is generally found to be more efficient and robust. In addition, the concept behind multiple shooting is in good agreement with the InterMoon Superhighway concept that uses unstable periodic orbits as waypoints in the chaotic space (see Figure 14). In fact, these resonant orbits can be used as starting points for the intermediate nodes of multiple shooting. This way, the resonant path of the controlled trajectory is preselected, and the solution is therefore encouraged to fall into the pass regions which lead to the desired resonance transport. In other words, the multiple shooting concept comes naturally from the understanding of the chaotic phase space structure of the problem. It is therefore expected to be efficient in overcoming the sensitivity of chaotic motion.

Controlling the trajectory is obtained through small impulsive tether maneuvers that are optimized by the solver. The multiple shooting optimization problem is formulated as a nonlinear parameter optimization sub-problem, where the control variables are the positions, time, magnitude and direction of the tether maneuvers. A first guess is generated using resonant periodic orbits (at appropriate energy levels). In this study, an in-house multiple shooting optimization tool, called OPTIFOR,[27] is adapted to design trajectories surfing the InterMoon Superhighway with tether maneuvers. This tool can take advantage of powerful modern nonlinear optimizers such as SNOPT or IPOPT.

C. Example of Tether-Assisted Tour

In this section, the efficiency of the Interplanetary Superhighway method is demonstrated by computing an optimal end-to-end trajectory from a Lyapunov orbit of the L1 point of Callisto to a Halo orbit of the L2 point of Europa, passing through Lyapunov orbits at Ganymede. This Callisto-Ganymede-Europa example is chosen because there is a lot of scientific interest in these three moons, and this problem is therefore relevant in the context of future Jovian missions. Table 4 gives specific values for the CR3BP parameters used in this paper for the Jupiter-Callisto, Jupiter-Ganymede and Jupiter-Europa systems.

Table 4. Jupiter-Callisto, Jupiter-Ganymede and Jupiter-Europa CR3BP parameters

CR3BP	Mass ratio	Orbital radius *LU* (km)	Orbital period *TU* (days)
Jupiter-Callisto	5.6681e-05	1882700	16.6902
Jupiter-Ganymede	7.8037e-05	1070337.37782	7.1543
Jupiter-Europa	2.5266e-05	671101.96385	3.5520

The first step is to select the Jacobi constants of the Lyapunov and resonant orbits for each three-body problem. These Jacobi constants are initially set to $C_{\_Callisto} = 3.0031$, $C_{\_Ganymede} = 3.0061$, and $C_{\_Europa} = 3.0016$. These energy levels are consistent with low-energy captures or escapes at the respective moons. In addition, the tether length is set to be 25 km.

The next step is to generate a good initial guess of the solution. On the Callisto dominant phase, the trajectory begins on a L1 Lyapunov orbit at Callisto and proceeds to the near-Hohmann orbit with the following sequence: L1 Lyapunov → Lyapunov Unstable Manifold → 5:6 → 4:5 → 7:9 → 3:4 → 8:11 → 5:7 → 7:10. The initial resonance 5:6 is chosen because it is the lowest resonance that can be reached by simply 'falling off' the Lyapunov orbit. The choice of the other resonances is the result of several trial-and-error optimizations to find a good resonant path. Similarly, the resonant path of the Ganymede exterior portion is (in backward time): L2 Lyapunov → Lyapunov Stable Manifold → 4:3 → 7:5 → 3:2. A quasi-ballistic heteroclinic connection (see section VI) is then computed for the transfer from a L2 Lyapunov orbit to a L1 Lyapunov orbit at Ganymede. The resonant path of the Ganymede interior portion is next: L1 Lyapunov → Lyapunov Unstable Manifold → 4:5 → 7:9 → 3:4 → 8:11. Finally, the resonant path of the Europa exterior portion is (in backward time): L2 Lyapunov → Lyapunov Stable Manifold → 5:4 → 9:7 → 4:3 → 11:8 → 7:5. For this overall transfer, there are therefore 20 moon flybys in total: 7 Callisto flybys, 8 Ganymede flybys, and 4 Europa flybys.

The optimization of this problem is performed using the OPTIFOR tool with the Intel Fortran compiler.[27] All constraints are enforced with a normalized tolerance of 10^{-8}, which corresponds to position and velocity discontinuities of around 10 m and 0.1 mm/s respectively. Targeting such a high tolerance is facilitated by the robust multi-shooting implementation.

The resulting optimized solution requires a total delta-v of 5 m/s only, and the total flight time is 1120 days, which is well within conceivable mission constraints. The small maneuvers are performed by the tether. The objective to find a propellantless transfer is therefore achieved, although in practice a small propulsive capability such as an attitude control engine will likely accompany the spacecraft and can also be used for minor translational control. We emphasize that the trajectory does include phasing and several fully integrated flybys of Callisto, Ganymede and Europa. The corresponding entire trajectory is shown in the inertial frame and in the rotating frames of the patched CR3BP model in Figure 15 - Figure 19. Time history of the orbital radius of the trajectory is given in Figure 20. We can see that the orbital radius is decreasing sequentially, as expected. First, the trajectory gets its perijove reduced with flybys of Callisto. Then, the spacecraft passes naturally to the control of Ganymede and accordingly reduces its apojove. Then the spacecraft travels to the interior resonances of Ganymede and gets its perijove reduced. Finally, the trajectory gets its apojove reduced with flybys of Europa. Example of the tether thrust profile is given in Figure 21 for the interior Ganymede-dominated portion. The required Lorentz force always stays below the maximum Lorentz force achievable by the tether.

Further insight of the dynamics is seen when plotting the spacecraft trajectory on the T-P graph, a new graphical tool introduced by Campagnola and Russell (see Figure 22).[28] On the T-P graph, level sets of constant Tisserand parameter are plotted in (r_a, r_p) space where the Tisserand parameter is almost equivalent to the Jacobi constant of the PR3BP. During the resonance hopping transfer, the spacecraft jumps between resonances (represented by big dots) along the level sets of Tisserand curves. Overall, the transfer orbit scarcely deviating from curves of constant Tisserand parameter, due to the small tether maneuvers.

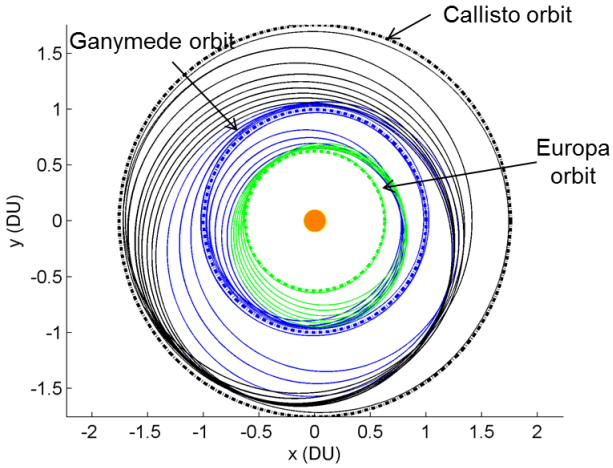

Figure 15. Low-energy tour in inertial frame (Black: Callisto-dominated; Blue: Ganymede-dominated; Green: Europa-dominated)

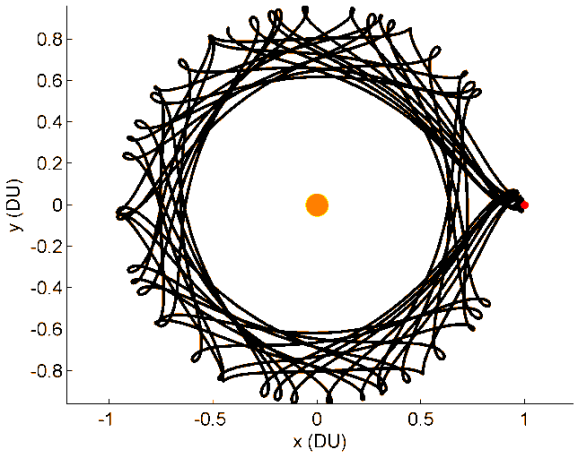

Figure 16. Callisto-dominated portion of the low-energy tour in Callisto rotating frame

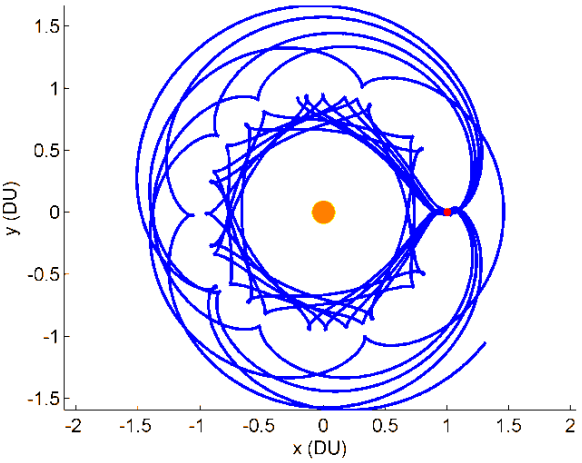

Figure 17. Ganymede-dominated portion of the low-energy tour in Ganymede rotating frame

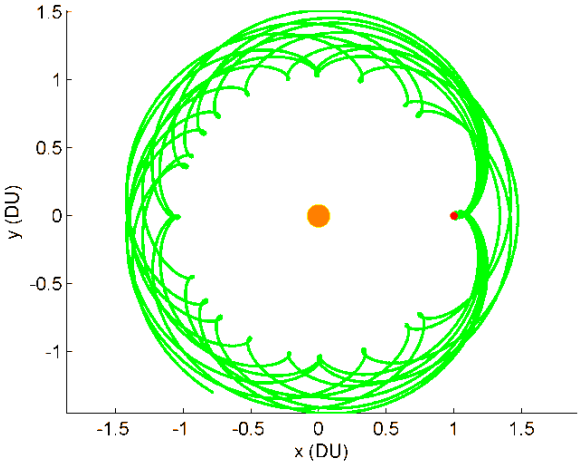

Figure 18. Europa-dominated portion of the low-energy tour in Europa rotating frame

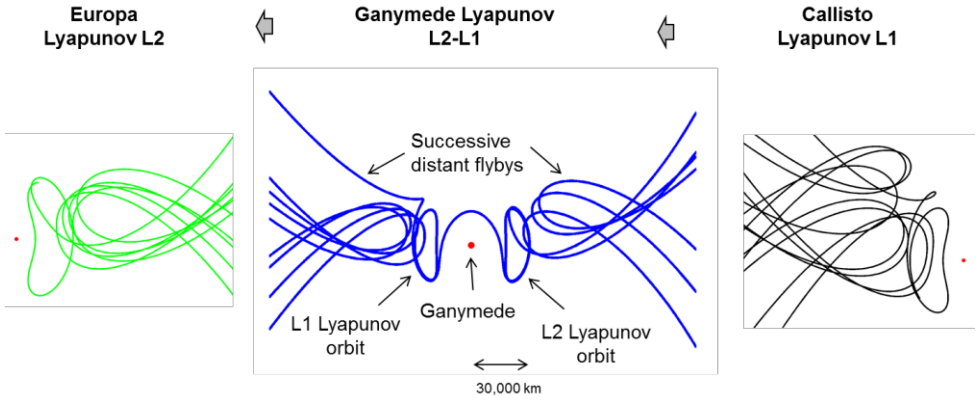

Figure 19. The low-energy tour is following the InterMoon Superhighway, passing through weakly captured Lyapunov orbits at the moons and performing high-altitude resonant flybys of the moons (Jupiter-Moon rotating frames)

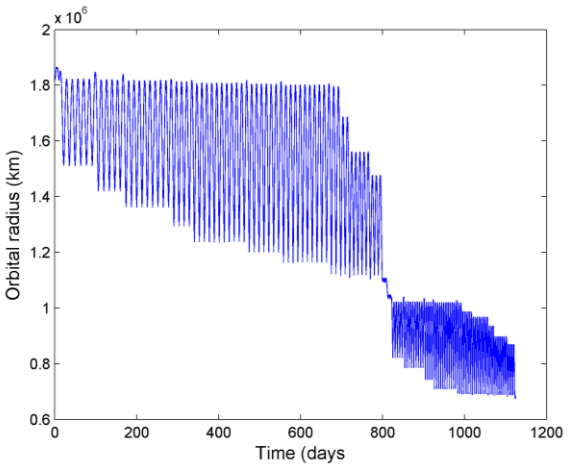

Figure 20. Time history of the orbital radius of the low-energy tour

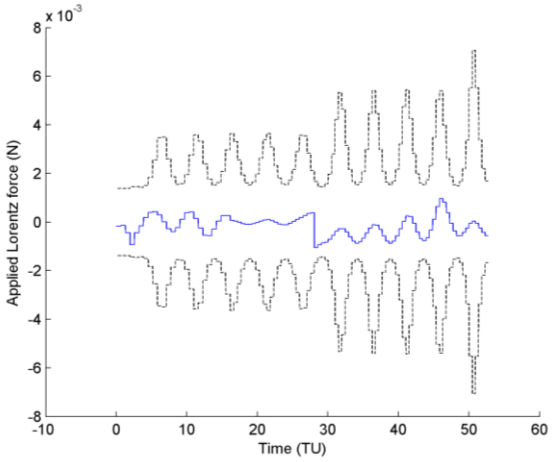

Figure 21. Lorentz force profile during interior Ganymede-dominated portion. Back dots represent the maximum Loretnz force that can be achieved by the tether

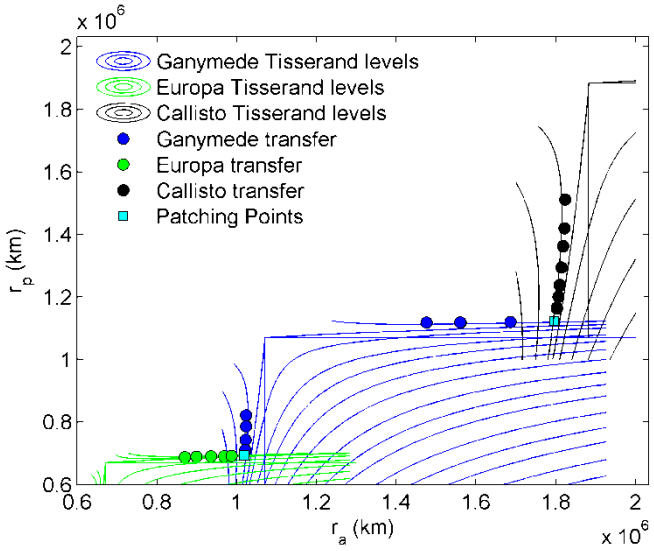

Figure 22. T-P graph of the low-energy tour

D. Radiation dose

Intense radiation, primarily from the trapped electron environment at Jupiter, poses a significant threat for the Magnetour. This section addresses that threat by defining the particle fluences for the mission trajectory and by using those fluences to estimate generic dose/depth curves. The latter are useful for modeling the required mass of shielding required to protect the mission electronic components to a desired survival level. This mass can then be traded-off against various mission scenarios. The mission segment covered in this study starts with the spacecraft in orbit at roughly Callisto's orbit distance and ends at Europa's orbit (this means that the solar proton event environment encountered on the way to Jupiter has been ignored — a safe assumption given that the dose from that portion of the trajectory is ~10% or less of the total expected dose…). Magnetour can save propellant mass by using a tether and gravity assists for orbit maneuvers. The tether will also supply electrical energy directly to the spacecraft. The trade-off is the enhanced radiation doses that the Magnetour will see because it spends long portions of the mission traversing the equatorial regions of the jovian radiation belts, where the radiation dose is maximized.

Radiation fluence (particle flux — number of particles per unit time — multiplied by exposure time along the trajectory) estimates are based on the GIRE 2 radiation model.[29] The Dose/depth curve is estimated using the NOVICE transport code.[30] The orbit information provided had random time steps between orbit points. This was

interpolated to give an orbit that had a constant 600 s time step. This is necessary for the Jupiter GIRE 2 program as it is presently coded. The resulting charged particle fluence estimates are shown in Figure 23.

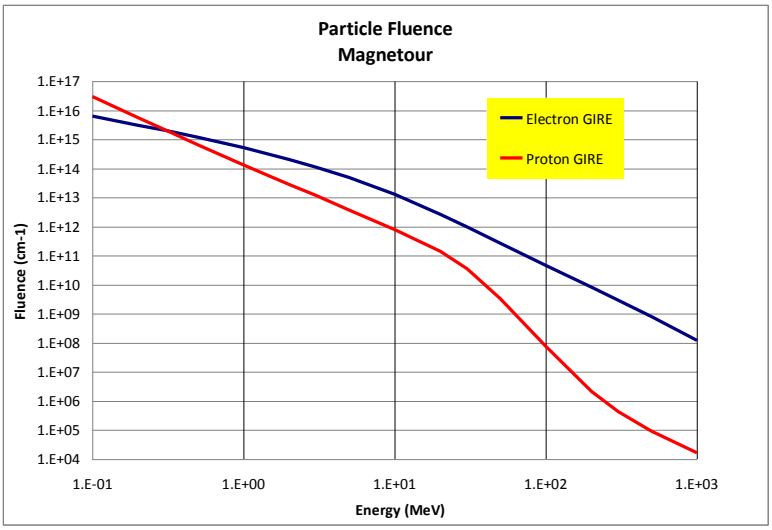

Figure 23. Particle fluences for the Magnetour mission

In addition to fluence, radiation dose involves the stopping power by a specified shielding material, typically aluminum, and the associated shield thickness of the material. Figure 24 gives the total radiation dose of Magnetour for a 4π spherical aluminum shell. For comparison purposes, the radiation doses for Juno and the Europa orbiter mission concept are also given.[31] These data provide the primary radiation information needed for the Magnetour mission study. As expected, radiation dose decreases with increasing shield thickness. The estimated TID ranges from ~5 Mrads behind the "canonical" 100 mils of aluminum shielding to ~100 krads for 1,000 mils (1,000 mils = 1 inch = 2.54 cm) of aluminum shielding. Interestingly, for a shielding thickness greater than 700 Mils Al, we can also observe that the radiation dose is similar with that predicted for the Europa Orbiter mission concept, which has similar scientific objectives at Europa – it is not orbiting any other moons though. The shielding thickess selected for the Europa orbiter mission concept is currently 700 Mils Al. If the same thickness is selected for Magnetour, our mission will experience similar radiation dose. Note that the Juno mission has dose levels ~10% of the Magnetour and Europa missions but it is in a roughly polar orbit and largely avoids the jovian moons and radiation belts.

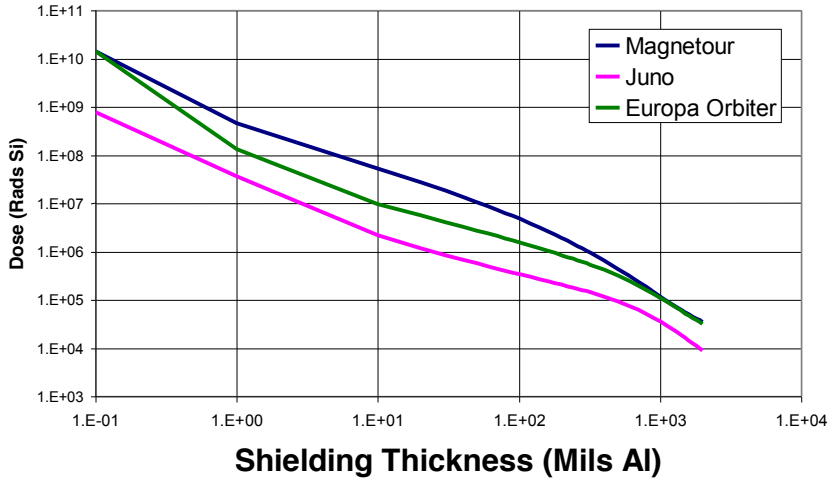

Figure 24. Total Dose Versus Shielding Thickness for Three Jupiter Missions. For > 700 Mils Al, radiation doses of Europa orbiter and Magnetour are equivalent

This result is quite surprising because Magnetour spends much more time in the radiation belt than Europa orbiter. It is necessary to look deeper into the radiation dose by species to understand this result (see Figure 25). For thin thicknesses, the dose comes from the proton environment. Europa Orbiter and Magnetour protons are approximately the same. After about one mil, the protons become less important as the electrons take over in dominating the dose, Magnetour has a higher electron fluence so it gets more dose until the two environments equalize at higher energies and the doses, once again, become the same. Note that the photons (bremsstrahlung) are becoming a problem around a few thousand mils because no extra shielding will be effective past that point.

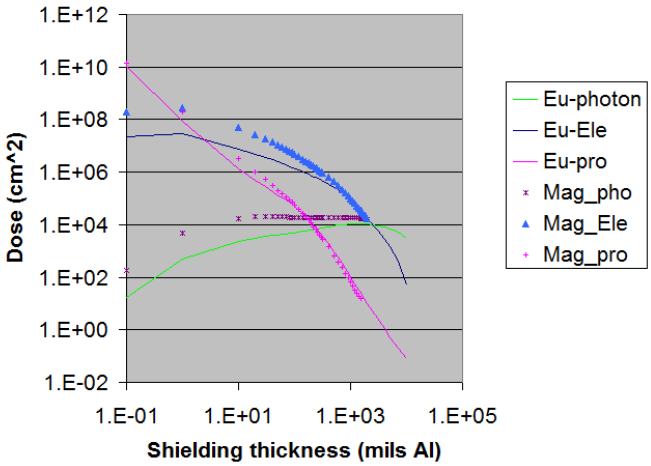

Figure 25. Total Dose Versus Shielding Thickness from protons, electrons and photons. Europa Orbiter environments are lines and Magnetour environments are symbols

VI. Weakly Captured Science Orbits

A. Lyapunov Orbits

Classical low altitude science orbits require expensive insertion maneuvers to enter deep into a large planetary moon's gravity well. The use of weakly captured periodic orbits is therefore suggested here,[3,32] with dramatically reduced insertion costs. In particular, interesting, planar, periodic families of orbits exist around the L1 and L2 libration points, and are referred to as Lyapunov orbits. They are often used as locations from which to make science observations of the secondary in the circular restricted three-body problem. Lyapunov orbits are unstable, and the instability may be quantified by computing the eigenvalues of the variational equations integrated once around the orbit (the monodromy matrix). If the eigenvalues are evaluated for the planar problem it may be seen that two will be unity, while another eigenvalue will be greater than one, and the final eigenvalue will be less than one. The stable and unstable directions may be obtained from the information contained within the monodromy matrix and used to compute the stable and unstable manifolds. These orbits are planar and are simpler to study. This analysis is therefore focused on these orbits.

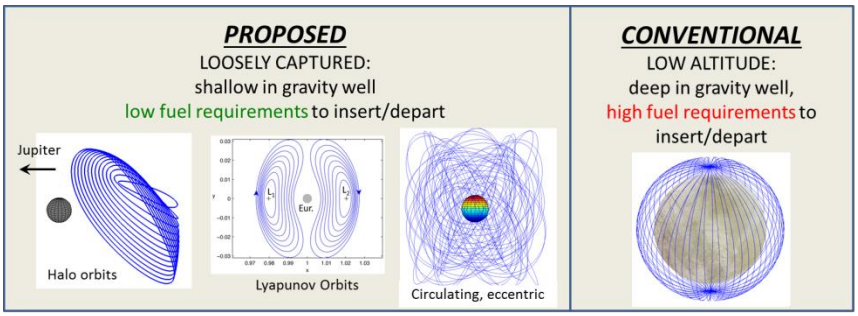

Figure 26. Science orbit options at the moons

Coupling magnetic and gravitational dynamics can also yield modified Lyapunov orbits that exhibit new and unique dynamical properties. In particular, the introduction of the tether force makes some periodic orbits stable in the typically unstable Lyapunov families. More details can be found in Ref. 2 and Ref. 33.

B. Heteroclinic Connections

Heteroclinic connections[34] are particularly useful for the Magnetour trajectory because they allow a transfer between two unstable periodic orbits for essentially no deterministic ΔV. This makes the use of these trajectories feasible because the spacecraft may still follow these trajectories despite the lack of an engine to provide the impulsive ΔVs required for traditional trajectories. In addition to this, they provide the potential for multiple close approaches with varying flyby conditions and viewing geometries that would be useful for science observations while providing wide coverage of the surface.

Heteroclinic connections are typically computed by searching for the intersection of the stable and unstable manifolds of these periodic orbits in a surface of section. Simply speaking, the stable manifold W^s of an unstable periodic orbit is composed of those trajectories that approach the orbit as time goes to infinity. The unstable manifold W^u of a periodic orbit is composed of those trajectories that approach that orbit as time goes to negative infinity. Mathematically these intersections are represented as:

$$W_{L1}^{u} \cap W_{L2}^{s}. \tag{7}$$

Invariant manifolds have been used to connect libration orbits before,[35,36] and heteroclinic connections have also been used with resonant orbits for tour and endgame design.[34,37-40] Additional specific uses have been found for transfers between orbits in the Sun-Earth and Earth-Moon systems,[41,42] and for cases in the elliptic-restricted problem with maneuvers.[43-47] They have also been further used to optimize transfers including maneuvers, and it has been found that they can speed to the design of transfers between trajectories (see Figure 19).[48]

Heteroclinic connections are explored here for particular scenarios involving connections between L1 and L2 in the Jupiter-Europa system. Many different heteroclinic connections may be computed, and one that is particularly interesting is the trajectory with a low altitude flyby of approximately 169.6 km near Europa in Figure 27a. These heteroclinic connections correspond to the intersections shown in the Poincaré section in Figure 27b. The Poincaré section shown here is computed using the surface of section Σ specified by x = 1 − μ shown in Figure 27a. It is a one-sided Poincaré section with $\dot{x} > 0$.

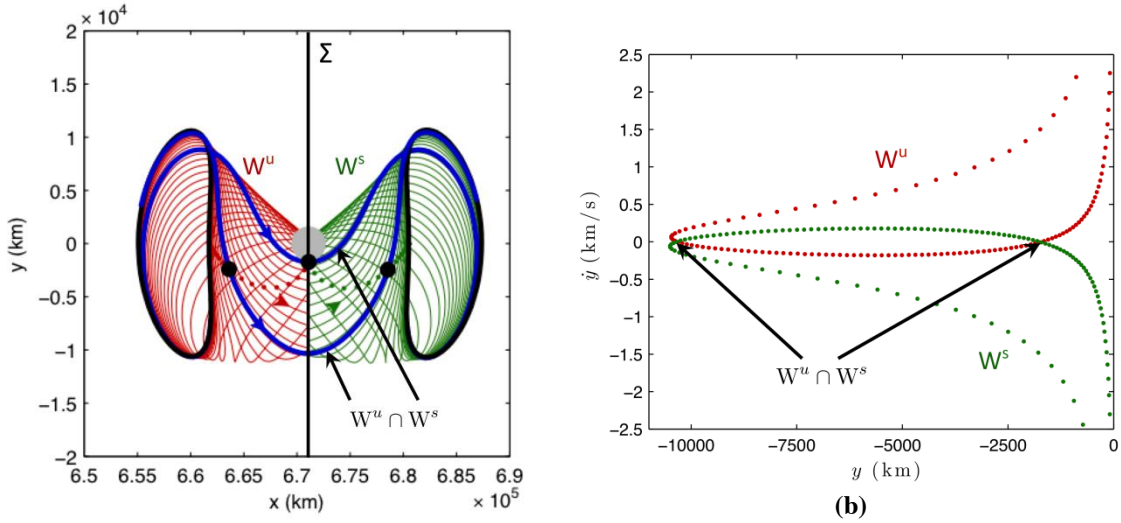

(a) (b)

Figure 27. (a) Heteroclinic connections computed from W^u_{L1} and W^s_{L2} at C = 3.0028. The black points indicate apses of the heteroclinic connections with respect to Europa while the small points on the invariant manifold trajectories correspond to apses on those trajectories. (b) Poincaré section showing W^u_{L1} and W^s_{L2} at C = 3.0028.

If additional observation opportunities are desired, heteroclinic connections with multiple loops around Europa may be computed. A sample trajectory that loops around Europa for C = 3.0031 may be computed by selecting a different Poincaré section. For the sample trajectory shown next the intersections were limited to those trajectories that intersect the surface of section twice, and the Poincaré section is one-sided in that $\dot{x} < 0$. The resulting Poincaré section is shown in Figure 28a. The intersection chosen here is the one near y ≈ 0.014 and $\dot{y} = 0$. The corresponding

trajectory plotted in position space is shown in Figure 28b. As can be seen from the plot, the trajectory travels completely around Europa once, and the apses relative to Europa are designated by points in the plot. These different apses give different close approach parameters for observations of the surface of Europa (Figure 29), and additional heteroclinic connections may be used to provide alternative observation sequences depending upon the science objectives. A direct transfer may also be computed between the two Lyapunov orbits as shown in the Poincaré section in Figure 30a. The actual trajectories corresponding to these intersections are shown in Figure 30b. Note that by the symmetry given by the transformation (x, y, $\dot{x}$, y; t) → (x, −y, $-\dot{x}$, $\dot{y}$, −t) inherent in the PCRTBP the reverse transfers are also known to exist.

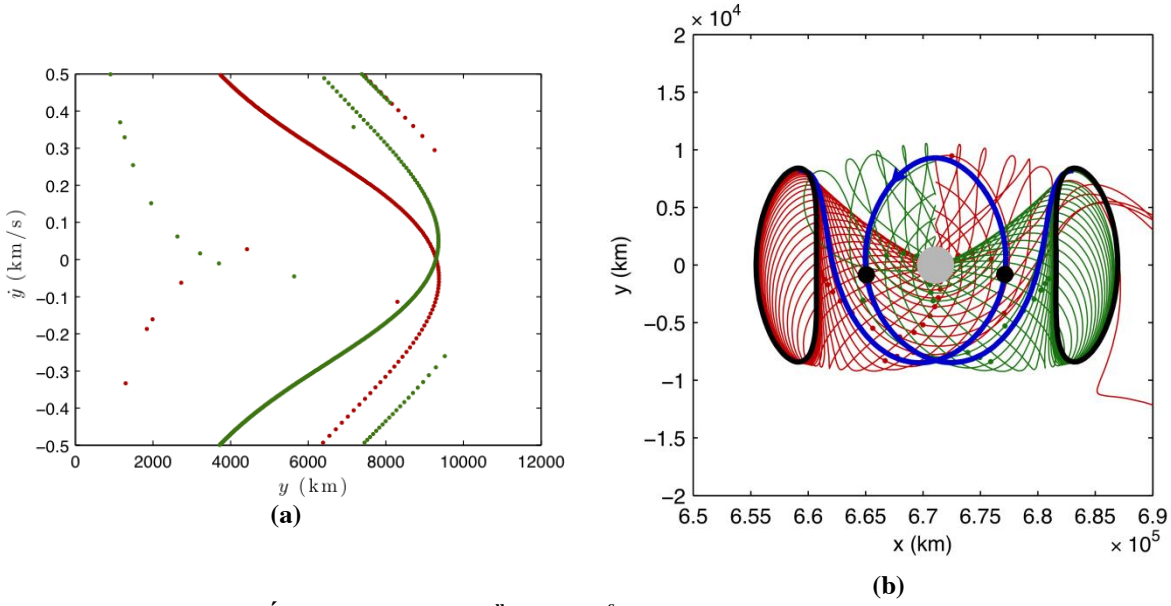

Figure 28. (a) Poincaré section showing W^u_{L1} and W^s_{L2} at C = 3.0031. (b) Heteroclinic connection that loops around Europa computed from W^u_{L1} and W^s_{L2} at C = 3.0031. The black points correspond to the apses of the heteroclinic connection, and the remaining points are the apses on the invariant manifolds of the libration orbits.

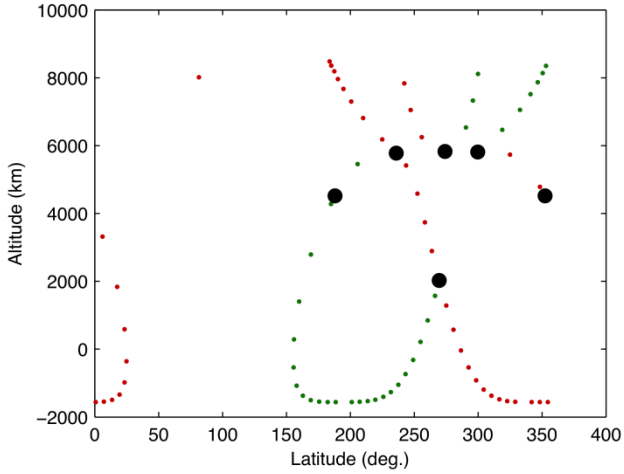

Figure 29. Periapse characteristics relative to Europa of all heteroclinic connections at C = 3.0031. The black points correspond to the apses of the heteroclinic connection, and the remaining points are the apses on the invariant manifolds of the libration orbits.

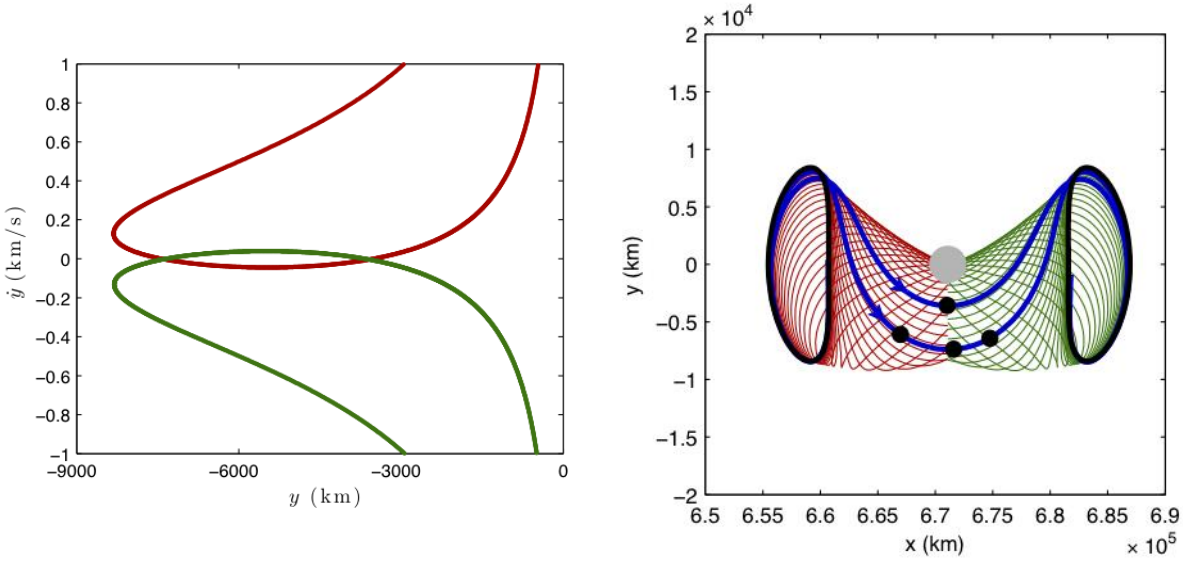

(a) **(b)**

Figure 30. (a) Poincaré section showing W^u_{L1} and W^s_{L2} at C = 3.0031. (b) Direct heteroclinic connection using W^u_{L1} and W^s_{L2} at C = 3.0031.

The results so far have demonstrated the potential utility of heteroclinic connections as a means to aid in science observations of a moon. They provide multiple apses around different points of the moon to provide fuller coverage of the moon than is possible from just the libration orbits or flybys. In the next phase a more detailed study of the benefits of these heteroclinic connections will be conducted. Additional heteroclinic connections at different energy levels will be found and analyzed. A search technique will also be implemented to search for additional heteroclinic connections around Europa including those with many passes around the moon that can help fill in any gaps in the science observations.

VII. Risks / Challenges

The space environment plays a critical role in the design of the Magnetour mission. The environment provides both the power and thrust for the mission. On the other hand, the environment, particularly the radiation environment, represents a significant risk/challenge for the electronic systems (and to a lesser extent the material properties). The major challenges posed by the environment are:

1) The TID ranges from ~5 Mrad(Si) behind 100 mils of Al, a low level of shielding, to ~100 Krads(Si), a very manageable dose level, behind ~1 inch of Al. Trade-offs in trajectory, careful shielding design (e.g., placing sensitive components inside a "vault"), and proper selection of rad-hard parts can help mitigate this high level shielding. Indeed, Galileo (a comparable mission scenario) was able to get by with an average of 2.2 g/cm^2 of shielding. Indeed, the tether itself can be coiled around sensitive areas in the more intense parts of the radiation belts (typically where the magnetic field is the highest so the length can be shorter) to provide variable shielding.

2) The dust/large particle environments associated with the planets' rings (e.g., Saturn's iconic rings) represent a potentially challenging risk of hypervelocity impact. In particular, a thin, traditional "wire" tether design represents and potentially huge area (very thin cross-section but an extreme length). As an example, a 1 cm diameter tether by 100 km represents a cross-section of 10^3 m^2 — a very large potential collisional cross-section. The "wire" tether would be sensitive to particle sizes of less than 1 cm diameter. The Magnetour mission will limit this risk by: A) Using a "tape" tether design (e.g., several cm wide but less than a cm thick to reduce mass requirements) which would require much larger, several cm diameter particles to break the tether. Typically there many less of these larger particles. B) Simply avoiding the regions where the particles are concentrates. Fortunately, at Jupiter, avoiding or limiting the exposure to the radial distances inside Io significantly limits this risk. Likewise, at Saturn, avoiding its rings inside ~3-44 Rs avoids the issue. Fortunately, the large satellites effectively "clean" out the orbits near them.

3) Spacecraft charging, surface, internal electrostatic discharge (IESD), and VxB are intrinsic to the tether design. The catastrophic discharge that destroyed the TSS-1 Shuttle tether experiment demonstrates the potential

VxB risk—high voltages and high currents. The methods for mitigating surface charging, IESD, and VxB effects, however, are well understood,[49] and standard mitigation techniques (e.g., proper grounding, partially conductive materials, etc.) will significantly limit these concerns.

VIII. Conclusion

In this paper, the novel mission architecture of Magnetour is developed, and its feasibility and applicability are investigated. Using numerical simulations that incorporate simplified orbital mechanics and tether dynamics, preliminary results suggest that a full propellantless Magnetour concept relying on electrodynamic tethers only is indeed feasible at Jupiter, using currently available tether materials. A low-energy tour surfing the InterMoon Superhighway and orbiting successively Callisto, Ganymede and Europa requires 5 m/s only (performed by a 25-km long tether), a dramatic improvement over classical patched-conics tour designs.

Propellantless propulsion technology offers enormous potential to transform the way NASA conducts outer planet missions. It is hoped that the Magnetour concept can replace heavy, costly, traditional chemical-based missions and can open up a new variety of trajectories around outer planets. Leveraging the powerful magnetic and multi-body gravity fields of planetary systems to travel freely among planetary moons would allow for long-term missions and provide unique scientific capabilities and flagship-class science for a fraction of the mass and cost of traditional concepts.

Acknowledgments

This study was funded in part by the NASA Innovative Advanced Concepts program, under announcement NNH12ZUA002N. Part of the research was carried out at the Jet Propulsion Laboratory, California Institute of Technology, under a contract with NASA. The authors would like to thank Maximilian Schadegg, Kevin Bokelmann, Damon Landau, Nathan Strange, and Daniel Grebow for their help on this project.

References

[1] "Visions and Voyages for Planetary Science in the Decade 2013 – 2022", National Research Council Report, 2011, http://solarsystem.nasa.gov/2013decadal/

[2] Lantoine, G., Anderson, R. L., Garrett, H. B., Katz, I., Landau, D., Russell, R. P., and Strange, N. J., "MAGNETOUR: Surfing Planetary Systems on Electromagnetic and Multi-Body Gravity Fields," NASA Innovative Advanced Concepts Final Rept., July 2013, pp. 1–103.

[3] Lantoine, G., Russell, R. P., "Near-Ballistic Halo-to-Halo Transfers Between Planetary Moons", Journal of the Astronautical Sciences, Vol. 58, No. 3, 2011, pp. 335-363.

[4] Kloster K. W., Petropoulos A. E., Longuski J. M., "Europa Orbiter tour design with Io gravity assists", Acta Astronautica, Vol. 68, pp. 931-946, 2011.

[5] Schadegg M. M., Russell R. P., Lantoine G., "Jovian Orbit Capture and Eccentricity Reduction Using Electrodynamic Tether Propulsion", Journal of Spacecraft and Rockets, Vol. 52, No. 2, pp. 506-516, 2015.

[6] Sanmartin, J. R., Martinez-Sanchez, M., and Ahedo, E., "Bare Wire Anodes for Electrodynamic Tethers", Journal of Propulsion and Power, Vol. 9, No. 3, 1993, pp. 353–360.

[7] Zanutto, D., Curreli, D., and Lorenzini, E.C., "Stability of Electrodynamic Tethers in a Three-Body System," Journal of Guidance, Control, and Dynamics, Vol. 34, No. 5, Sept.-Oct. 2011, pp.1441-1456.

[8] Cooke, D. L., and Katz, I., "TSS-1R electron currents: Magnetic limited collection from a heated presheath", Geophysical Research Letters, Vol. 25, No. 5, pp. 753-756, 1998.

[9] Katz, I., Lilley Jr., J. R., Greb, A., McCoy, J. E., Galofaro, J., Ferguson, D. C., "Plasma turbulence enhanced current collection: Results from the plasma motor generator electrodynamic tether flight", Journal of Geophysical Research, Vol. 100, No. A2, pp. 1687-1690, 1995.

[10] Giorgini, J.D., Yeomans, D.K., Chamberlin, A.B., Chodas, P.W., Jacobson, R.A., Keesey, M.S., Lieske, J.H., Ostro, S.J., Standish, E.M., Wimberly, R.N., "JPL's On-Line Solar System Data Service", Bulletin of the American Astronomical Society, Vol 28, No. 3, p. 1158, 1996.

[11] Divine, T. N., and Garrett, H. B., "Charged particle distributions in Jupiter's magnetosphere," J. Geophys. Res., vol. 88, pp. 6889-6903, 1983.

[12] Khan B., Sanmartin J. R., "A comparative analysis of survival probability of round wire and thin-tape tethers of equal mass and length against debris impact", 39th COSPAR Scientific Assembly. Held 14-22 July 2012, in Mysore, India. Abstract B0.2-35-12, p.918.

[13] Kruijff, M., van der Heide, E. J., Stelzer, M., Ockels,W. J., and Gill, E.,"First Mission Results of the YES2 Tethered SpaceMail Experiment,"AIAA Paper 08-7385, Aug. 2008.

[14] Fujii, H.A., Watanabe, T., Kojima, H., Oyama,K., Kusagaya T., Yamagiwa, Y., Ohtsu, H., Cho, M., Sasaki, S., Tanakaka, K., Williams, J., Binyamin, R., Les Johnson, C., Khazanov, G., Sanmartin, J.R., Lebreton, J-P., van der Heide, J.E., Kruijff, M.,

Pascal,F., and Trivailo, P., “Sounding rocket experiment of bare electrodynamic tether system”, Elsevier, Acta Astronautica, Vol.64, pp. 313-324, 2009.
[15] Personnal correspondence with Dan Goebel.
[16] Peck M. A., “Prospects and Challenges for Lorentz-Augmented Orbits”, 2005 AIAA Guidance, Navigation, and Control Conference and Exhibit, San Francisco, CA, USA, 15-18 Aug. 2005.
[17] Janhunen, P., “Electric Sail for Spacecraft Propulsion,” Journal of Propulsion and Power, Vol. 20, No. 4, 2004, pp. 763–764.
[18] Janhunen, P., and Sandroos, A., “Simulation Study of Solar Wind Push on a Charged Wire: Basis of Solar Wind Electric Sail Propulsion,” Annales Geophysicae, Vol. 25, No. 3, 2007, pp. 755–767.
[19] Mengali G., Quarta A. A., and Janhunen P.. "Electric Sail Performance Analysis", Journal of Spacecraft and Rockets, Vol. 45, No. 1 (2008), pp. 122-129.
[20] Frisbee, R. H., “Advanced Space Propulsion for the 21st Century”, Journal of Propulsion and Power, Vol. 19, No. 6, 2003, pp.1129-1154.
[21] Lantoine G., Russell R. P., Campagnola S., “Optimization of Low-Energy Resonant Hopping Transfers between Planetary Moons,” Acta Astronautica, Vol. 68, No. 7-8, 2011, doi:10.1016/j.actaastro.2010.09.021.
[22] Russell R. P., Lam T., “Designing Ephemeris Capture Trajectories at Europa using Unstable Periodic Orbits,” Journal of Guidance, Control, and Dynamics 30 (2) (2007) 482–491.
[23] Ross S. D., Koon W. S., Lo M. W., Marsden J. E., “Design of a multi-moon orbiter,” Paper AAS03-143, AAS/AIAA Space Flight Mechanics Meeting, Ponce, PuertoRico, February 2003.
[24] Koon W. S., Lo M. W., Marsden J. E., Ross S. D., “Constructing a low energy transfer between jovian moons,” *Contemporary Mathematics*, 292 (2002)129–145.
[25] Ross S. D., Scheeres D. J., “Multiple Gravity Assists, Capture, and Escape in the Restricted Three-body Problem,” *SIAM J. Applied Dynamical Systems*, 6 (3) (2007) 576–596.
[26] Schroer C. G., Ott E., “Targeting hamiltonian systems that have mixed regular / chaotic phase spaces”, Chaos:An Interdisciplinary Journal of Nonlinear Science, 7(4), 1997, 512–519.
[27] Lantoine, G., Russell, R. P., A Unified Framework for Robust Optimization of Interplanetary Trajectories, Paper AIAA-2010-7828, AAS/AIAA Astrodynamics Specialist Conference and Exhibit, Toronto, Canada, Aug 2010.
[28] Campagnola, S., Russell, R. P., The Endgame Problem Part 2: Multi-Body Technique and T-P graph, Journal of Guidance, Control, and Dynamics, Vol. 33, No. 2, 2010, pp. 476-486, DOI 10.2514/1.44290
[29] Garrett, H. B., I. Jun, J. M. Ratliff, R. W. Evans, G. A. Clough, and R. W. McEntire, "Galileo Interim Radiation Electron Model," JPL Publication 03-006, The Jet Propulsion Laboratory, California Institute of Technology, Pasadena, CA, 2003.
[30] Jordan, T., “NOVICE: A Radiation Transport shielding code”, 2006.
[31] Europa 2012 Study Report (Unlimited Release), 2012.
[32] Russell, R. P., Brinckerhoff, A.T., “Circulating Eccentric Orbits around Planetary Moons”, Journal of Guidance, Control, and Dynamics. Vol. 32, No. 2, 2009, pp. 423-435.
[33] Bokelmann K. A., Russell R. P., Lantoine G., “Periodic Orbits and Equilibria Near Jovian Moons Using an Electrodynamic Tether”, Journal of Guidance, Control, and Dynamics, Vol. 38, No. 1, pp. 15-29, 2015.
[34] Anderson, R. L. and M. W. Lo, “Flyby Design using Heteroclinic and Homoclinic Connections of Unstable Resonant Orbits,” *21st AAS/AIAA Space Flight Mechanics Meeting*, AAS 11-125, New Orleans, Louisiana, February 13-17, 2011.
[35] Gomez G., Koon W. S., Lo M. W., Marsden J. E., and Ross S. D., “Connecting Orbits and Invariant Manifolds in the Spatial Restricted Three-Body Problem,” Nonlinearity, Vol. 17, May, 2004, pp. 1571– 1606.
[36] Gomez G. and Masdemont J., “Some Zero Cost Transfers between Libration Point Orbits,” AAS/AIAA Astrodynamics Specialist Conference, No. AAS Paper 00-177, Clearwater, Florida, January 23-26, 2000.
[37] Anderson R. L. and Lo M. W., “Role of Invariant Manifolds in Low-Thrust Trajectory Design,”Journal of Guidance, Control, and Dynamics, Vol. 32, November-December, 2009, pp. 1921–1930.
[38] Anderson R. L. and Lo M. W., “Dynamical Systems Analysis of Planetary Flybys and Approach: Planar Europa Orbiter,” Journal of Guidance, Control, and Dynamics, Vol. 33, November-December, 2010, pp. 1899–1912.
[39] Anderson R. L. and Lo M. W., “A Dynamical Systems Analysis of Planetary Flybys and Approach: Ballistic Case,” The Journal of the Astronautical Sciences, Vol. 58, April-June, 2011, pp. 167–194.
[40] Anderson R. L., “Tour Design Using Resonant Orbit Heteroclinic Connections in Patched Circular Restricted Three-Body Problems,” 23rd AAS/AIAA Space Flight Mechanics Meeting, No. AAS 13-493, Kauai, Hawaii, February 10-14, 2013.
[41] Canalias E. and Masdemont J., “Homoclinic and Heteroclinic transfer Trajectories Between Lyapunov Orbits in the Sun-Earth and Earth-Moon Systems,” Discrete and Continuous Dynamical Systems – Series A, Vol. 14, February, 2006, pp. 261–279.
[42] Canalias E. and Masdemont J., “Computing Natural Transfers Between Sun-Earth and Earth-Moon Lissajous Libration Point Orbits,” Touching Humanity - Space for Improving Quality of Life. Selected Proceedings of the 58th International Astronautical Federation Congress, Vol. 63, Hyderabad, India, 24-28 September 2007 2008, pp. 238 – 248.
[43] Hiday-Johnston L. A. and Howell K. C., “Transfers Between Libration-Point Orbits in the Elliptic Restricted Problem,” Celestial Mechanics and Dynamical Astronomy, Vol. 58, April 1994, pp. 317– 337.
[44] Hiday-Johnston L. A. and Howell K. C., “Impulsive Time-Free Transfers Between Halo Orbits,”Celestial Mechanics and Dynamical Astronomy, Vol. 64, 1996, pp. 281–303.
[45] Hiday L. A. and Howell K. C. “Impulsive Time-Free Transfers Between Halo Orbits,” AIAA/AAS Astrodynamics Conference, No. AIAA-92-4580, Hilton Head Island, South Carolina, August 10-12, 1992.

[46] Hiday L. A., Optimal Transfers Between Libration-Point Orbits in the Elliptic Restricted Three-Body Problem. PhD thesis, Purdue University, August 1992.
[47] Howell K. C. and Hiday-Johnston L. A., "Time-Free Transfers Between Libration-Point Orbits in the Elliptic Restricted Problem," Acta Astronautica, Vol. 32, No. 4, 1994, pp. 245–254.
[48] Lantoine G., Russell R. P., Campagnola S., "Optimization of Low-Energy Resonant Hopping Transfers between Planetary Moons," Acta Astronautica, Vol. 68, No. 7-8, 2011, doi:10.1016/j.actaastro.2010.09.021.
[49] Garrett, H. B., and Whittlesey, A. C., "Guide to Mitigating Spacecraft Charging Effects", *JPL Space Science and Technology Series*, J. H. Yuen, Editor-in-Chief, John Wiley and Sons, Inc., Hoboken, NJ, 221 pages, 2011.